NANO LETTERS

Letter

pubs.acs.org/NanoLett

Chloride Molecular Doping Technique on 2D Materials: WS_2 and MoS_2

Lingming Yang,[†] Kausik Majumdar,[‡] Han Liu,[†] Yuchen Du,[†] Heng Wu,[†] Michael Hatzistergos,[§] P. Y. Hung,[‡] Robert Tieckelmann,[‡] Wilman Tsai,[∥] Chris Hobbs,[‡] and Peide D. Ye*,[†]

[†]School of Electrical and Computer Engineering and Birck Nanotechnology Center, Purdue University, West Lafayette, Indiana 47907, United States

[‡]SEMATECH, Albany, New York 12203, United States

[§]College of Nanoscale Science and Engineering, State University of New York at Albany, Albany, New York 12203, United States

[∥]Intel Corporation, Santa Clara, California 95054, United States

Supporting Information

ABSTRACT: Low-resistivity metal−semiconductor (M−S) contact is one of the urgent challenges in the research of 2D transition metal dichalcogenides (TMDs). Here, we report a chloride molecular doping technique which greatly reduces the contact resistance (R_c) in the few-layer WS_2 and MoS_2. After doping, the R_c of WS_2 and MoS_2 have been decreased to 0.7 kΩ·μm and 0.5 kΩ·μm, respectively. The significant reduction of the R_c is attributed to the achieved high electron-doping density, thus a significant reduction of Schottky barrier width. As a proof-of-concept, high-performance few-layer WS_2 field-effect transistors (FETs) are demonstrated, exhibiting a high drain current of 380 μA/μm, an on/off ratio of 4×10^6, and a peak field-effect mobility of 60 $cm^2/(V \cdot s)$. This doping technique provides a highly viable route to diminish the R_c in TMDs, paving the way for high-performance 2D nanoelectronic devices.

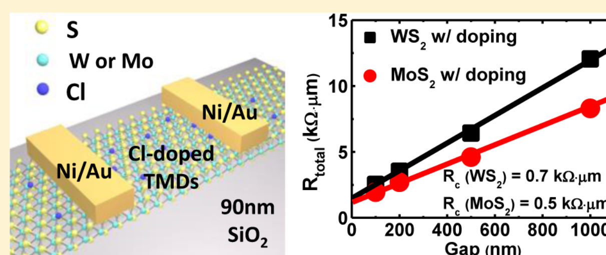

KEYWORDS: *molecular doping, WS_2, MoS_2, TMDs, contact resistance, Schottky barrier*

Recently, 2D TMD materials have trigged intensive research interests due to their unique electrical,[1,2] optical,[3] and mechanical properties.[4] MoS_2, one of the most studied TMD materials, has been used as the channel material of the FET, exhibiting high on/off ratio and high mobility.[5−9] Recent studies on the transistor characteristics of MoS_2 FETs reveal that the MoS_2 transistors are essentially Schottky barrier transistors whose switching is controlled by the tuning of the Schottky barrier at the contacts.[10] The model of Schottky barrier transistor also holds true in other TMD materials such as $MoSe_2$,[11] WS_2,[12] and WSe_2.[13] For Schottky barrier transistors, the intrinsic properties of the TMDs channel are masked by the Schottky contacts and no merits are gained from aggressive scaling.[14] In order to deal with the Schottky contact issue in TMDs, intensive research efforts have been made in recent years. A lot of attention has been paid to various contact metals including Sc,[15] In,[13] Al,[13,16] Ti,[10,13,15,17] Cr,[8] Mo,[18] Ni,[11,15,19] Au,[7,16] and Pt.[15,16] Unfortunately, most of these metal−semiconductor (M−S) contacts showed non-negligible Schottky barriers regardless of the contact metals.[16] Among them, some studies showed interesting results by engineering the contact metal. For instance, the Sc-MoS_2 contact shows a very low M−S interface resistance (0.65 kΩ·μm). However, the overall R_c is still considered to be large (∼5 kΩ·μm) due to the semiconductor internal resistance.[15] Other studies were aimed to metalize the TMDs under the contact by forming chemical bonds between sulfur and contact metal. W. Liu et al. reported an R_c of 0.8 kΩ·μm in Ti-15-layers-MoS_2 but the R_c of Ti-1-layer-MoS_2 is as large as 740 kΩ·μm.[17] In general, it is difficult to achieve a low R_c in TMDs by simply using contact metals with low work functions because the Fermi-level tends to be pinned at charge neutrality level (CNL) or S-vacancy level which is located below the conduction band edge with non-negligible Schottky barrier heights.[20,21] To make things worse, it is even more difficult to achieve low R_c in other TMD materials (such as WS_2) because their CNLs are located in the middle of the bandgap[22,23] with larger Schottky barriers for electrons compared with MoS_2.[12]

Another key way to achieve the low R_c on the M−S contact is to heavily dope the semiconductor under the metal.[24] After heavy doping, the Schottky barrier width is reduced and current through the M−S contact is greatly enhanced by electron tunneling. The doping process is achieved by dopant diffusion or ion-implantation in traditional semiconductors. For the atomically thin semiconductors, it is a challenge to precisely control the doping density with the ion-implantation because

Received: July 10, 2014
Revised: October 1, 2014
Published: October 13, 2014

ACS Publications © 2014 American Chemical Society

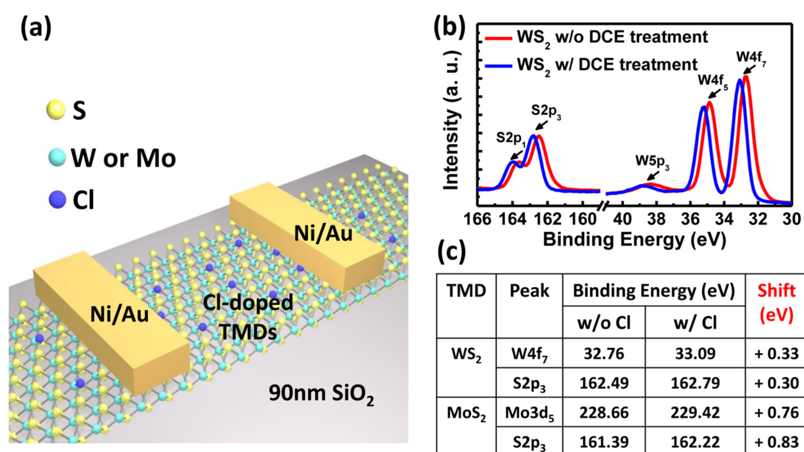

TMD	Peak	Binding Energy (eV)		Shift (eV)
		w/o Cl	w/ Cl	
WS_2	$W4f_7$	32.76	33.09	+ 0.33
	$S2p_3$	162.49	162.79	+ 0.30
MoS_2	$Mo3d_5$	228.66	229.42	+ 0.76
	$S2p_3$	161.39	162.22	+ 0.83

Figure 1. (a) Schematic of Cl-doped few-layer WS_2 back-gate FET. The chemical doping is achieved by soaking the flakes in the 1,2-dichloroethane (DCE) solution for more than 12 h and rinsed by acetone and isopropanol for 30 min. The contact metal Ni (30 nm)/Au (60 nm) is deposited immediately after the e-beam lithography. Back gate oxide is 90 nm SiO_2 and p^{+2} Si is used as back gate contact. (b) The binding energies of core levels in WS_2 with and without the DCE treatment. Blue shifts of the peak were observed after DCE treatment. (c) Summarize of the shifts of the binding energy in WS_2 and MoS_2 before and after DCE treatment. The energy peaks shows about +0.3 eV shifts and +0.8 eV shifts in WS_2 and MoS_2, respectively.

the thickness of the semiconductor is only a few nanometers.[25] On the other hand, new doping techniques, such as molecular doping, show the potential advantages over ion-implantation when applied to the ultrathin 2D semiconductors. H. Fang et al. used potassium[26] as an adatom dopant to reduce the R_c in WSe_2 and MoS_2. Du et al. also explored to apply PEI molecular doping to reduce the R_c in MoS_2.[27] However, the aforementioned two methods have limited improvement in the R_c and also doping effect degrades with time. In this Letter, we report a novel chloride molecular doping method on TMD materials. After doping, the R_c of Ni-WS_2 and Ni-MoS_2 contacts has been significantly reduced to 0.7 kΩ·μm and 0.5 kΩ·μm, respectively. High doping density of 6.0×10^{11} cm^{-2} and 9.2×10^{12} cm^{-2} are achieved on the few-layer WS_2 and MoS_2 at zero back gate biases. XPS results reveal that the high doping densities are attributed to the doping by Cl. In addition, high performance few-layer WS_2 FETs have been demonstrated with a drain current of 380 μA/μm, an I_{on}/I_{off} ratio $>4 \times 10^6$, and a peak field-effect mobility of 60 $cm^{-2}/(V\cdot s)$. No degradation of I_{on}/I_{off} ratio is observed after the doping. The results show that the chloride molecular doping method is a promising way to achieve low R_c in TMD materials.

Results and Discussion. Figure 1a schematically shows the structure of Cl-doped few-layer WS_2 or MoS_2 back gate FETs. The fabrication process starts with the mechanical exfoliation of bulk WS_2 (Nanosurf Inc.) and bulk MoS_2 (SPI supplies) using scotch tape method. The exfoliated WS_2 or MoS_2 flakes are transferred onto a 90 nm SiO_2/p^{+2} Si wafer and then soaked in undiluted 1, 2 dichloroethane (DCE) (99.8%, SIGMA-Aldrich, No. 34872) at room temperature for more than 12 h. The thickness is about 3.5 to 5 nm (5−7 monolayer) which is first identified by optical microscope and measured by atomic force microscopy (AFM). Using thin flake (1−4 layers) will lead to higher contact resistance due to the increasing of the bandgap (see the Supporting Information). Acetone and isopropanol rinses are performed to remove the residual chemical. E-beam lithography is used to define the contact region with a fixed contact width of 1 μm. Transfer length method (TLM) structures with various gap spaces are designed to extract the R_c. The combination of Ni (30 nm)/Au (60 nm) is deposited as contact metals by e-beam evaporator at the pressure of 2×10^{-6} Torr. The electrical measurements are carried out with Keithley 4200 Semiconductor Parameter Analyzer.

In order to verify the n-type doping, X-ray photoelectron spectroscopy (XPS) surface analysis is used to measure the Fermi levels in TMDs before and after the DCE treatment. As shown in Figure 1b, blue shifts (increase in energy) are observed in the binding energy of core levels in WS_2 after the DCE treatment. Because the binding energy of XPS spectra is referenced to Fermi level in the material, the blue shifts of binding energy can be interpreted by the move up of the Fermi level in the semiconductor. Figure 1c summarizes the energy shifts of core levels in WS_2 and MoS_2. For WS_2, the binding energy of W $4f_7$ shifts from 32.76 to 33.09 eV, whereas the peak of S $2p_3$ shifts from 162.49 to 162.79 eV; for MoS_2, the binding energy of Mo $3d_5$ shifts from 228.66 to 229.42 eV while S $2p_3$ shifts from 161.39 to 162.22 eV. An increment of about 0.3 and 0.8 eV in binding energy was observed in DCE treated WS_2 and MoS_2, respectively. It should be noticed that a larger shift of the binding energy in MoS_2 does not necessarily correspond to a larger shift of the Fermi level in it as the time lag between DCE treatment and XPS is different for two cases. The stability of the Cl-doped MoS_2 and WS_2 FETs can be seen in the Supporting Information. On the other hand, the threshold voltage of WS_2 and MoS_2 FETs exhibit a negative shift after DCE treatment. The negative shift of threshold voltage indicates there is a higher electron density in the semiconductor channels with DCE treatment. As a result, it is reasonable to conclude that the n-type doping is achieved by the DCE treatment. The doping mechanism on TMDs by the DCE treatment is not completely established yet. One possible mechanism is that the substitute doping of the TMDs is realized through the replacement of S vacancy by Cl atom. It has been reported that none of the element of halogen family is an effective dopant when acts as an adatom dopant.[28] However, previous simulation shows that when high density sulfur atoms are substituted by Cl atoms the discrete impurity energy levels in MoS_2 broaden into a band and merge with conduction band, resulting the band gap narrowing and the degeneration doping.[29] On the other hand, it was also observed that a significant amount of Cl element was

detected on the flakes' surface by secondary ion mass spectrometry (SIMS) even though the TMD materials are thoroughly rinsed by acetone and isopropanol.[30] Given that sulfur vacancies are widely detected from the mineral MoS_2,[21] it is reasonably assuming that the doping effect is achieve by the extra electrons donated by Cl atoms when they occupy the location of sulfur vacancies.

The R_c of WS_2 and MoS_2 can be significantly reduced after the Cl doping. Known as an ambipolar semiconductor, the undoped WS_2 shows large Schottky barriers for both electrons and holes, resulting an extremely large R_c.[12] For such a larger Schottky barrier, it would be impractical to extract the R_c by the TLM structure which is applicable to Ohmic or low resistivity contacts only. However, a simple estimation of the R_c of the undoped WS_2 is on the order of 10^2 kΩ·μm because the total resistance of the 100 nm device is calculated to be 5×10^2 kΩ·μm. After doping, an R_c as low as 0.7 kΩ·μm, 2−3 orders of magnitude reduction, can be extracted by linearly fitting the curve of total resistances. Figure 2a shows the TLM resistances

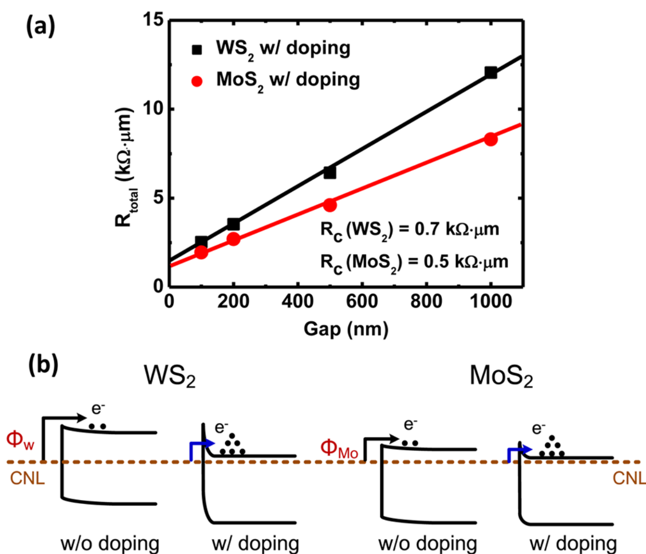

Figure 2. (a) TLM resistances of Cl-doped WS_2 and MoS_2. The R_c is extracted to be 0.7 kΩ·μm and 0.5 kΩ·μm at the back gate bias of 50 V for WS_2 and MoS_2, respectively. For WS_2, the L_T is extracted to be 132 nm and the corresponding ρ_c is about 9.2×10^{-6} Ω·cm^2 and the doping density is about 6.0×10^{11} cm^{-2}. For MoS_2, the L_T is 60 nm and the ρ_c is about 3×10^{-7} Ω·cm^2 and the doping density is about 9.2×10^{12} cm^{-2}. (b) Schematic band diagram of metal-TMD contacts with and without chloride doping. Before DCE treatment, the Fermi level is pinned close to the CNL, resulting a large Schottky barrier. After DCE treatment, WS_2 and MoS_2 are heavily doped and the Fermi level in 2D materials can be efficiently moved after the passivation of S vacancy by Cl dopants.

of the Cl-doped WS_2 and MoS_2 as a function of gap space at a back gate bias of 50 V. The corresponding transfer length (L_t) of Cl-doped WS_2 is about 132 nm extracted from the TLM. The specific contact resistivity ($\rho = R_c L_T W$) is calculated to be 9.2×10^{-6} Ω·cm^2, where W is the channel width. The sheet doping density in WS_2 is about 6.0×10^{11} cm^{-2} determined by the equation of

$$n = \frac{L}{eWR_{sh}\mu}$$

where L is the channel length, e is the electron charge, R_{sh} is the sheet resistance, and μ is the field-effect mobility shown in Figure 4a. To the best of our knowledge, such a low R_c has never been achieved on WS_2 or other TMDs whose CNL is located in the middle of the bandgap. On the other hand, an even lower R_c of 0.5 kΩ·μm was obtained on Cl doped MoS_2. Compared with the R_c of the undoped MoS_2 (about 5−6 kΩ·μm),[19] a ten times reduction has also been achieved after doping.[30] The ρ_c and the doping density of Cl-doped MoS_2 are determined to be 3×10^{-7} Ω·cm^2 and 9.2×10^{12} cm^{-2}, respectively.

The mechanism of the reduction of the R_c on Cl-doped TMDs is very clear. The energy band diagrams of the Ni-WS_2 and Ni-MoS_2 contacts with and without the Cl doping are shown in Figure 2b. The Fermi level at the metal-WS_2 interface is pinned near the CNL, resulting a significantly large Schottky barrier. The barrier height is given by

$$\Phi = \lambda_{gs}(\Phi_m - \chi_s) + \Phi_0(1 - \lambda_{gs})$$

[31] where λ_{gs} is gap states parameter, Φ_m is the metal work function, χ_s is the electron affinity of the semiconductor, and Φ_0 is the charge neutrality position. The height of the Schottky is large enough to rectify the electrons' ejection from the metal to the semiconductor at low V_{ds}, as shown in Figure 2b. Moreover, this barrier height cannot be efficiently modified by varying the workfunction of contact metals due to the complicated metal-to-TMD interface.[21] The difference of the R_c between WS_2 and MoS_2 is due to the difference alignment of the CNL in the two materials.[22,32] Compared with MoS_2, the CNL in WS_2 is more close to the middle of the bandgap, resulting a larger Schottky barrier. Without doping, it would be much harder for the electrons to inject from the metal to the semiconductor in WS_2 because the thermionic current exponentially decreases with the increasing of barrier height. However, when the tunneling current starts to dominate the current through the M−S junction, the electron injection through the barrier becomes much easier. The effective electron density (induced by chemical doping and electrostatic doping) at V_{bg} of 50 V is as high as 2.3×10^{13} cm^{-2} and 2.9×10^{13} cm^{-2} for WS_2 and MoS_2, respectively. As a result, both of the R_c in the WS_2 and MoS_2 decrease significantly after doping. However, it is interesting that most of the electron density in WS_2 is attributed to the back gate bias rather the chemical doping. In other words, the Fermi level (electron density) at the interface can be effectively modulated by the back gate bias. Effective modulation via field-effect can be ascribed to the passivation of sulfur vacancy by Cl, given that the sulfur vacancy is the cause of the Fermi level pining on MoS_2 and WS_2 at M−S interface.[20] The hysteresis of the $I-V$ characteristics due to the doping ions has also been discussed in the Supporting Information.

It is reasonable to predict that the molecular doping method would also be valid in other TMDs as long as there are vacancies of chalcogenide elements. The reduction of the R_c by the doping technique is extremely important for TMDs whose Fermi level is pinned close to the mid bandgap. Due to the relative low Schottky barrier, MoS_2 has been given overwhelming attentions in recent years. However, for most of the TMDs, their intrinsic properties have not be fully investigated because they are hidden by the large R_c.[10] By effectively reducing the R_c, the molecular doping technique can be applied to other TMDs research. Applying low work function metal Ti is not successful. We ascribe the failure to the fact that Ti is a getter which deteriorates the substitute doping of Cl.

Because the low R_c is achieved in WS_2 by Cl doping, high-performance WS_2 FET is expected. The output characteristics of the Cl-doped few-layer WS_2 FETs with 100 nm channel length are shown in Figure 3a. The device exhibits promising device performance including a drain current of 380 μA/μm as well as good current saturation. Due to a small R_c, the linear region of the $I_{ds}-V_{ds}$ curves shows excellent linearity. The drain current starts to saturate at V_{ds} of 1.0 V due to the electron velocity saturation. Figure 3b shows the $I_{ds}-V_{ds}$ curves of the 100 nm WS_2 FET without Cl doping, which is used as a control device. Obvious rectify characteristics are observed at the low drain bias (<0.5 V), indicating a large Schottky barrier at the contact. Compared with undoped devices, the drive current of the Cl-doped WS_2 FET has been improved by more than six times. Figure 3c shows the transfer curves of the Cl-doped few-layer WS_2 FET with 100 nm channel length. Due to a relative large band gap and ultrathin-body-on-insulator structure, the off-current is as low as 10^{-10} μA/μm and 10^{-12} μA/μm at drain biases of 2 and 0.05 V, respectively. The low off-state current is attractive for low power applications especially when the device works at the ultrascaled gate length. The I_{on}/I_{off} ratio is about 4×10^6 and 3×10^7 at the drain bias of 2 and 0.05 V, respectively. Compared with the undoped WS_2 FET in Figure 3d, the I_{on}/I_{off} ratio has been increased 2-fold due to the improvement of the on-current. By the linearly extrapolating of $I_{ds}-V_{gs}$ curves, the threshold voltage is calculated to be −14 and 1.7 V for the doped and undoped devices, respectively. The negative shift of the threshold voltage is due to the n-type doping in channel. Unlike other doping methods which use charge transfer from absorbed molecules or atoms such as PEI

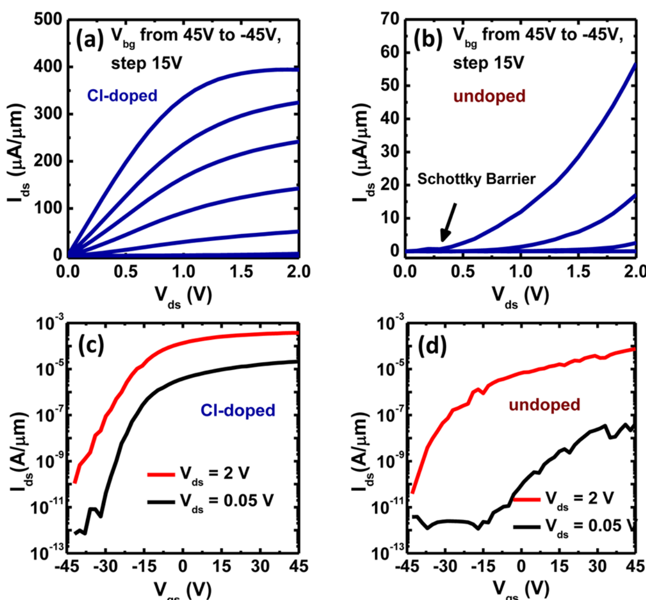

Figure 3. (a) Output characteristics of the Cl-doped few-layer WS_2 FETs at 100 nm channel length. The maximum drain current is enhanced to 380 μA/μm after Cl doping. Excellent current saturation is also observed. (b) Output characteristics of the undoped few-layer WS_2 FETs. The drain current is significantly suppressed by the Schottky barrier, indicating a larger barrier height. (c) Transfer characteristics of the device in panel a. The off-current is as low as 10^{-10} μA/μm and 10^{-12} μA/μm at V_{ds} of 2 and 0.05 V. The I_{on}/I_{off} ratio is about 4×10^6 and 3×10^7 at V_{ds} of 2 and 0.05 V, respectively. (d) Transfer characteristics of the device in panel b. The I_{on}/I_{off} ratio is about 2×10^6 and 1.1×10^4 at V_{ds} of 2 and 0.05 V.

and potassium, the off-current of the Cl-doped FETs do not exhibit any degradation even at 100 nm short channel length. This result also indicates that the doping procedure is not fulfilled by the surface adhesion of extra atoms or molecules, otherwise there would be a leakage current through the doping layer. The good device performance of Cl-doped WS_2 FETs shows that the presented chloride molecular doping techniques is a powerful method to be applied to dope the TMDs and fabricate high performance 2D FETs.

We have also investigated the scaling down trends of the Cl-doped WS_2 FETs, including the field-effect mobility, I_{on}/I_{off} ratio and the drive current. Previously, the field-effect mobility of WS_2 was significantly underestimated due to the large Schottky barrier.[12,31] As shown in Figure 4a, the field-effect mobility is carefully calculated by subtracting the R_c at different back gate bias. The mobility is given by

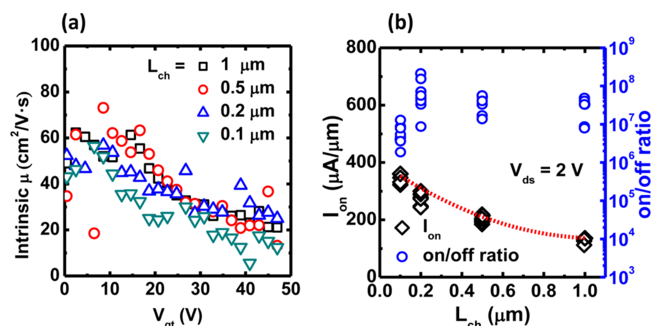

Figure 4. (a) The field-effect motilities as a function of the back gate bias for the WS_2 FETs with various channel lengths. The peak mobility is about 60 $cm^2/(V \cdot s)$, which is close to the Hall mobility. (b) I_{on}/I_{off} ratio and maximum drain current of Cl-doped few-layer WS_2 FETs as a function of channel length. For channel length >0.2 μm, the I_{on}/I_{off} ratio is more than 1×10^7; for 100 nm channel length device, the I_{on}/I_{off} ratio decreases due to the loss of gate control. The drive current increases from 136 μA/μm to 380 μA/μm with the channel length scales down from 1 to 0.1 μm.

$$\mu = \left(\frac{L}{WC_{ox}}\right)\frac{d}{d(V_{bg} - V_{th})}\left(\frac{1}{R_{tot} - 2R_c}\right)$$

where W and L are the channel width and length, respectively, C_{ox} is the oxide capacitance, V_{bg} is the back gate bias, V_{th} is the threshold voltage, R_{tot} is the total resistance, $2R_c$ is the total contact resistance. The peak field-effect mobility is about 60 $cm^2/(V \cdot s)$, which is similar to the values in the Cl-doped MoS_2 FETs.[30] Considering the high doping density in channel, the motilities are among the good values in TMD materials. When the device is at high electron density region, the electron mobility decreases to around 20 $cm^{-2}/(V \cdot s)$. At both the high V_{bg} and low V_{bg} regions, the obtained field-effect motilities agree well with the reported Hall mobility measured with ion liquid gate.[33] The scaling down trends of the drain currents of 0.1, 0.2, 0.5, 1 μm devices are shown in Figure 4b. The on-current increases from 136 μA/μm to 380 μA/μm with the channel length scales down from 1 to 0.1 μm. Figure 4b also shows the I_{on}/I_{off} ratio for devices with different channel lengths. For long channel devices, the I_{on}/I_{off} ratios are more than 3×10^7. The I_{on}/I_{off} ratio increases with the channel length scaling due to the increasing of the maximum drain current. For 100 nm devices, the off-current increases because of the drain-induced-barrier-lowering. As the result, the I_{on}/I_{off} ratio

decreases to 4×10^6. Considering the thick gate oxide (90 nm SiO_2), it is reasonable to observe the degradation of the gate electrostatic control of the channel at the short gate length. If a thinner and high-*k* gate dielectric were used, a higher on/off ratio can be achieved. Previously, Cl-doped few-layer MoS_2 FETs have been demonstrated to have a low R_c of 0.5 kΩ·μm, a high drain current of 460 μA/μm, and a high on/off ratio of 6.3 $\times$ 10^5.[30] Compared with MoS_2, Cl-doped WS_2 FETs exhibit comparable low R_c, high drain current, and field-effect mobility. The advantages of WS_2 FETs over MoS_2 ones are the low off-state current and the high on/off ratio.

Conclusion. In summary, a novel chloride molecular doping technique is demonstrated on WS_2 and MoS_2. The R_c of Ni-WS_2 and Ni-MoS_2 contacts have been reduced to 0.7 kΩ·μm and 0.5 kΩ·μm with the presented technique. The significant improvement in R_c is due to the n-type doping thus the reduction of the Schottky barrier width. The doping mechanism could be the occupation of sulfur vacancies by chlorine atoms rather than the surface adhesion of chloride molecules. High performance few-layer WS_2 FETs have been successfully demonstrated using Cl doping. The 100 nm WS_2 FET has a high drain current of 380 μA/μm, a high on/off ratio of 4×10^6, and a field-effect mobility around 60 $cm^2/(V \cdot s)$. In addition, no degeneration of I_{on}/I_{off} ratio is observed after the Cl doping. The scaling down characteristics of the Cl-doped WS_2 FETs have also been investigated. Compared with Cl-doped MoS_2 FETs, Cl-doped WS_2 FETs show comparable electrical performance and better on/off ratio. This doping technique can also be widely applied to other TMD materials to achieve low R_c and provide a route to realize high-performance electronic devices with 2D materials.

ASSOCIATED CONTENT

Supporting Information

thickness dependence of the Cl-doped MoS_2/WS_2 FETs, hysteresis data, and stability of the device in vacuum and air. This material is available free of charge via the Internet at http://pubs.acs.org.

AUTHOR INFORMATION

Corresponding Author

*E-mail: yep@purdue.edu. Tel.: 1-765-494-7611. Fax: 1-765-496-7443.

Notes

The authors declare no competing financial interest.

ACKNOWLEDGMENTS

The work at Purdue University is supported by SEMATECH and SRC. The authors would like to thank Hong Zhou, Yexin Deng, and Zhe Luo for the valuable discussions and technical assistance.

REFERENCES

(1) Mak, K. F.; Lee, C.; Hone, J.; Shan, J.; Heinz, T. F. Atomically Thin MoS_2: A New Direct-Gap Semiconductor. *Phys. Rev. Lett.* **2010**, *105* (13), 136805.

(2) Novoselov, K. S.; Jiang, D.; Schedin, F.; Booth, T. J.; Khotkevich, V. V.; Morozov, S. V.; Geim, A. K. Two-Dimensional Atomic Crystals. *Proc. Natl. Acad. Sci. U.S.A.* **2005**, *102* (30), 10451−10453.

(3) Sundaram, R. S.; Engel, M.; Lombardo, A.; Krupke, R.; Ferrari, A. C.; Avouris, P.; Steiner, M. Electroluminescence in Single Layer MoS_2. *Nano Lett.* **2013**, *13* (4), 1416−1421.

(4) Bertolazzi, S.; Brivio, J.; Kis, A. Stretching and Breaking of Ultrathin MoS_2. *ACS Nano* **2011**, *5* (12), 9703−9709.

(5) Liu, H.; Neal, A. T.; Ye, P. D. Channel Length Scaling of MoS_2 MOSFETs. *ACS Nano* **2012**, *6* (10), 8563−8569.

(6) Majumdar, K.; Hobbs, C.; Kirsch, P. D. Benchmarking Transition Metal Dichalcogenide MOSFET in the Ultimate Physical Scaling Limit. *IEEE Electron Device Lett.* **2014**, *35* (3), 402−404.

(7) Radisavljevic, B.; Radenovic, A.; Brivio, J.; Giacometti, V.; Kis, A. Single-Layer MoS_2 transistors. *Nat. Nanotechnol.* **2011**, *6* (3), 147−150.

(8) Wang, H.; Yu, L.; Lee, Y.-H. H.; Shi, Y.; Hsu, A.; Chin, M. L.; Li, L.-J. J.; Dubey, M.; Kong, J.; Palacios, T. Integrated Circuits Based on Bilayer MoS_2 Transistors. *Nano Lett.* **2012**, *12* (9), 4674−4680.

(9) Yoon, Y.; Ganapathi, K.; Salahuddin, S. How Good Can Monolayer MoS_2 Transistors Be? *Nano Lett.* **2011**, *11* (9), 3768−3773.

(10) Liu, H.; Si, M.; Deng, Y.; Neal, A. T.; Du, Y.; Najmaei, S.; Ajayan, P. M.; Lou, J.; Ye, P. D. Switching Mechanism in Single-Layer Molybdenum Disulfide Transistors: An Insight into Current Flow across Schottky Barriers. *ACS Nano* **2013**, *8* (1), 1031−1038.

(11) Larentis, S.; Fallahazad, B.; Tutuc, E. Field-Effect Transistors and Intrinsic Mobility in Ultra-Thin $MoSe_2$ Layers. *Appl. Phys. Lett.* **2012**, *101* (22), 223104.

(12) Sik Hwang, W.; Remskar, M.; Yan, R.; Protasenko, V.; Tahy, K.; Doo Chae, S.; Zhao, P.; Konar, A.; Xing, H.; Seabaugh, A.; Jena, D. Transistors with Chemically Synthesized Layered Semiconductor WS_2 exhibiting 10^5 Room Temperature Modulation and Ambipolar Behavior. *Appl. Phys. Lett.* **2012**, *101* (1), 013107.

(13) Liu, W.; Kang, J.; Sarkar, D.; Khatami, Y.; Jena, D.; Banerjee, K. Role of Metal Contacts in Designing High-Performance Monolayer n-Type WSe_2 Field Effect Transistors. *Nano Lett.* **2013**, *13* (5), 1983−1990.

(14) Liu, H.; Si, M.; Najmaei, S.; Neal, A. T.; Du, Y.; Ajayan, P. M.; Lou, J.; Ye, P. D. Statistical Study of Deep Submicron Dual-Gated Field-Effect Transistors on Monolayer Chemical Vapor Deposition Molybdenum Disulfide Films. *Nano Lett.* **2013**, *13* (6), 2640−2646.

(15) Das, S.; Chen, H.-Y. Y.; Penumatcha, A. V.; Appenzeller, J. High Performance Multilayer MoS_2 Transistors with Scandium Contacts. *Nano Lett.* **2013**, *13* (1), 100−105.

(16) Walia, S.; Balendhran, S.; Wang, Y.; Ab Kadir, R.; Sabirin Zoolfakar, A.; Atkin, P.; Zhen, O. J.; Sriram, S.; Kalantar-zadeh, K.; Bhaskaran, M. Characterization of Metal Contacts for Two-Dimensional MoS_2 Nanoflakes. *Appl. Phys. Lett.* **2013**, *103* (23), 232105.

(17) Wei, L.; Jiahao, K.; Wei, C.; Sarkar, D.; Khatami, Y.; Jena, D.; Banerjee, K. High-Performance Few-Layer-MoS_2 Field-Effect-Transistor with Record Low Contact-Resistance. *IEEE International Electron Devices Meeting (IEDM)*; IEEE: New York, 2013; p 19.14.11.

(18) Kang, J.; Liu, W.; Banerjee, K. High-Performance MoS_2 Transistors with Low-Resistance Molybdenum Contacts. *Appl. Phys. Lett.* **2014**, *104* (9), 093106.

(19) Liu, H.; Neal, A. T.; Du, Y.; Ye, P. D. Fundamentals in MoS_2 Transistors: Dielectric, Scaling and Metal Contacts. *ECS Trans.* **2013**, *58* (7), 203−208.

(20) Liu, D.; Guo, Y.; Fang, L.; Robertson, J. Sulfur Vacancies in Monolayer MoS_2 and Its Electrical Contacts. *Appl. Phys. Lett.* **2013**, *103* (18), 183113.

(21) McDonnell, S.; Addou, R.; Buie, C.; Wallace, R. M.; Hinkle, C. L. Defect-Dominated Doping and Contact Resistance in MoS_2. *ACS Nano* **2014**, *8* (3), 2880−2888.

(22) Kang, J.; Tongay, S.; Zhou, J.; Li, J.; Wu, J. Band Offsets and Heterostructures of Two-Dimensional Semiconductors. *Appl. Phys. Lett.* **2013**, *102* (1), 012111.

(23) Gong, C.; Zhang, H.; Wang, W.; Colombo, L.; Wallace, R. M.; Cho, K. Band alignment of two-dimensional transition metal dichalcogenides: Application in tunnel field effect transistors. *Appl. Phys. Lett.* **2013**, *103* (5), 053513.

(24) Yu, A. Y. C. Electron Tunneling and Contact Resistance of Metal-Silicon Contact Barriers. *Solid-State Electron.* **1970**, *13* (2), 239−247.

(25) Pelaz, L.; Duffy, R.; Aboy, M.; Marques, L.; Lopez, P.; Santos, I.; Pawlak, B. J.; van Dal, M.; Duriez, B.; Merelle, T.; Doornbos, G.; Collaert, N.; Witters, L.; Rooyackers, R.; Vandervorst, W.; Jurczak, M.; Kaiser, M.; Weemaes, R. G. R.; van Berkum, J.; Breimer, P.; Lander, R. Atomistic Modeling of Impurity Ion Implantation in Ultra-Thin-Body Si Devices. *IEEE International Electron Devices Meeting (IEDM)*; IEEE: New York, 2008; pp 1−4.

(26) Fang, H.; Tosun, M.; Seol, G.; Chang, T. C.; Takei, K.; Guo, J.; Javey, A. Degenerate n-Doping of Few-Layer Transition Metal Dichalcogenides by Potassium. *Nano Lett.* **2013**, *13* (5), 1991−1995.

(27) Du, Y.; Liu, H.; Neal, A. T.; Si, M.; Ye, P. D. Molecular Doping of Multilayer MoS_2 Field-Effect Transistors: Reduction in Sheet and Contact Resistances. *IEEE Electron Device Lett.* **2013**, *34* (10), 1328−1330.

(28) Dolui, K.; Rungger, I.; Das Pemmaraju, C.; Sanvito, S. Possible Doping Strategies for MoS_2 Monolayers: An Ab Initio Study. *Phys. Rev. B* **2013**, *88* (7), 075420.

(29) Sun, Q.-Q.; Li, Y.-J.; He, J.-L.; Yang, W.; Zhou, P.; Lu, H.-L.; Ding, S.-J.; Wei Zhang, D. The Physics and Backward Diode Behavior of Heavily Doped Single Layer MoS_2 Based p−n Junctions. *Appl. Phys. Lett.* **2013**, *102* (9), 093104.

(30) Yang, L. M. K.; Du, Y.; Liu, H.; Wu, H.; Hatzistergos, M.; Hung, P.; Tieckelmann, R.; Tsai, W.; Hobbs, C.; Ye, P. D., High-Performance MoS_2 Field-Effect Transistors Enabled by Chloride Doping: Record Low Contact Resistance (0.5 k$\Omega\cdot\mu$m) and Record High Drain Current (460 μA/μm). *Symposia on VLSI Technology and Circuits (VLSI 2014)*; VLSI, 2014; pp.192−193.

(31) Tung, R. T. Chemical Bonding and Fermi Level Pinning at Metal-Semiconductor Interfaces. *Phys. Rev. Lett.* **2000**, *84* (26), 6078−6081.

(32) Jiang, H. Electronic Band Structures of Molybdenum and Tungsten Dichalcogenides by the GW Approach. *J. Phys. Chem. C* **2012**, *116* (14), 7664−7671.

(33) Braga, D.; Gutiérrez Lezama, I.; Berger, H.; Morpurgo, A. F. Quantitative Determination of the Band Gap of WS_2 with Ambipolar Ionic Liquid-Gated Transistors. *Nano Lett.* **2012**, *12* (10), 5218−5223.